THE JOURNAL OF PHYSICAL CHEMISTRY Letters

Letter

pubs.acs.org/JPCL

Hexagonal BC_3: A Robust Electrode Material for Li, Na, and K Ion Batteries

Rajendra P. Joshi, Burak Ozdemir, Veronica Barone,* and Juan E. Peralta

Department of Physics and Science of Advanced Materials, Central Michigan University, Mount Pleasant, Michigan 48859, United States

Supporting Information

ABSTRACT: We have investigated the stability, maximum intercalation capacity, and voltage profile of alkali metal intercalated hexagonal BC_3 (M_xBC_3), for $0 < x \leq 2$ and M = Li, Na, and K. Our calculations, based on dispersion-corrected density functional theory, show that these intercalation compounds are stable with respect to BC_3 and their bulk metal counterparts. Moreover, we found that among all M_xBC_3 considered, the maximum stable capacity corresponds to an x value of 1.5, 1, and 1.5 for Li, Na, and K, respectively. These values are associated with large gravimetric capacities of 572 mA h/g for Na and 858 mA h/g for Li and K. Importantly, we show that metal intercalated hexagonal BC_3 has the advantage of a small open-circuit voltage variation of approximately 0.49, 0.12, and 0.16 V for Li, Na, and K, respectively. Our results suggest that BC_3 can become a robust alternative to graphitic electrodes in metal ion batteries, thus encouraging further experimental work.

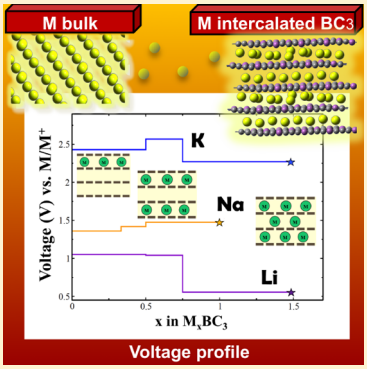

The fast-growing impact of batteries in modern technology is well-documented.[1−3] Metal ion battery technologies have evolved significantly, yet their application for high-density storage is limited in part due to the lack of high-energy-density electrodes. This limitation encourages the search of new electrode materials that can meet the demand for high-energy-density applications. Significant attention has been placed across a wide range of materials for the development of efficient electrodes for metal ion batteries such as graphite,[4−7] graphene oxides,[8] layered transition-metal sulfides,[9] transition-metal oxides,[10−12] metal alloys,[13] and transition-metal carbides.[14]

Alkali metal intercalated graphite and its derivatives have been extensively investigated both theoretically[15−18] and experimentally[19−21] owing to its low cost, chemical stability, and reversible capacity for absorbing and releasing metal ions between its galleries. Moreover, graphite has been widely adopted as an anode material in commercially available lithium ion batteries (LIBs) due to its high energy and power densities.[2] However, due to the increasing demand of Li and its limited abundance,[22] it is expected that LIBs alone cannot meet the needs of the rapidly growing battery market.

In this scenario, sodium ion batteries (NIBs) and potassium ion batteries (KIBs) are of particular interest[23−26] for energy storage applications due to the wide availability and low cost of these metals.[22] In recent years, considerable effort has been made to extend the technology of Li intercalation materials to Na and K. However, the difficulty of Na intercalation in graphitic anodes prohibits its use in battery applications.[26] Although at their early stages of development NIBs show promise, their applicability relies on finding proper electrode materials with suitable energy and power densities. To this end, several materials have been explored such as layered transition-metal oxides,[24] hard carbon,[25] sodium−tin alloys,[27] layered sulfides,[28] and transition-metal fluorides.[29,30]

In the search of suitable electrode materials for NIBs and KIBs, it is natural to look at their performance for Li intercalation as well. Xu et al.[31] predicted theoretically that hexagonal lithium borocarbide (LiBC) sheets can act as a reversible intercalation host for LIBs with improved Li intake capacity. LiBC has also attracted a lot of attention due to its remarkably high energy density of 1088 W h/kg and volumetric energy density of 2463 W h/L with high mobility of Li ions compared to that in graphite.[32−34] After the experimental realization of Li intercalated boron-doped graphite in 1995,[35] some theoretical works were devoted to studying the electrochemical properties of Li intercalated BC_3.[32,33] However, these works do not consider the staging mechanism and voltage profile diagrams of Li intercalation in BC_3. It is expected that the electron deficiency with respect to graphite introduced by the high content of B in BC_3 will render it suitable not only for Li intercalation but, importantly, for Na and K as well. Alkali metal intercalation in BC_3 has been experimentally demonstrated by Kouvetakis et al.,[36] yet their electrochemical properties are still unknown. In this work, we have systematically studied the stability, maximum intercalation capacity, and voltage profile of Li, Na, and K intercalation in BC_3. To this end, we have employed dispersion-corrected density functional theory calculations and explicitly considered the staging mechanism that takes place in the intercalation process in order to obtain maximum theoretical capacities of metal

Received: May 27, 2015
Accepted: June 23, 2015
Published: June 23, 2015

DOI: 10.1021/acs.jpclett.5b01110
J. Phys. Chem. Lett. 2015, 6, 2728−2732

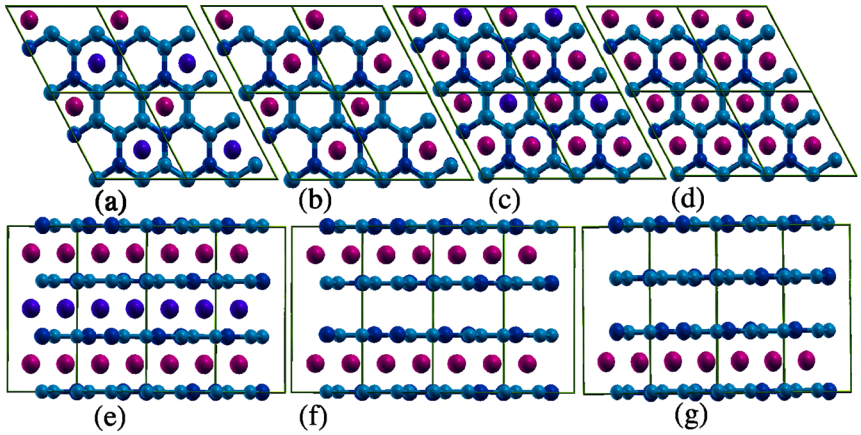

Figure 1. Scheme of the different intercalation structures studied in this work. The top row shows the [001] view of the 2 × 2 supercell of BC_3 for the different stoichiometries considered, showing the ordering of the metal atoms in between its layers (a) $M_{0.5}BC_3$, (b) M_1BC_3, (c) $M_{1.5}BC_3$, and (d) M_2BC_3. The side view (bottom row) shows the stage-I to stage-III metal arrangement, (e) stage-I, (f) stage-II, and (g) stage-III. Metal atoms at the top and bottom layers are shown in pink, while metals at the central layer are shown in purple for visualization purposes only; C atoms are shown in light blue and B atoms in blue.

intercalation. Density functional theory calculations have been performed using plane wave basis set and pseudopotentials as implemented in Quantum-ESPRESSO.[37] Dispersion interactions are taken into account by using the van der Waals exchange−correlation functional vdW-DF2-C09.[38]

During the charging and discharging process, it is expected to observe different stages as the metal concentration is gradually increased.[36] This staging has been experimentally observed in graphite[39,40] and has also been theoretically investigated.[17] The staging mechanism in graphite-like materials can be rationalized by considering the competition between ion−ion Coulomb repulsion and interlayer van der Waals attraction. If the energy corresponding to the Coulomb repulsion between metal ions is smaller than the energy required to expand the interlayer separation (governed by attractive van der Waals forces), then metal atom intercalation into a single gallery is favored until it reaches the maximum intercalation capacity before starting to fill adjacent empty galleries. For this work, we consider three intercalation stages (I−III). Four different concentrations of metal atoms (M) are considered for the stage-I intercalation (all galleries occupied) of BC_3, which can form M_xBC_3, with x values of 0.5, 1.0, 1.5, 2.0 (M = Li, Na, and K). In addition to stage-I structures, two more stages are examined, stage-II and -III, where stage-n corresponds to the structure with adjacent n − 1 empty galleries. The scheme of M_xBC_3 structures and the three different stages considered in our calculations are shown in Figure 1.

As in graphite, there are different possible stackings of the layers of BC_3. Therefore, we first determined the most stable stacking of pristine BC_3. Our calculations show that there are two structures that differ in energy at less than 5 meV/atom. The lowest-energy structure is an AB stacking type, similar to graphite. The second-lowest in energy structure is an AA stacking type in which B atoms in one layer sit on top of C atoms in the immediate next layer. The most stable stacking for metal intercalated BC_3, however, corresponds to the AA stacking. In all of the relative energy calculations presented here, we adopt the AA stacking as the reference for pristine BC_3. For all of the intercalated compounds, our calculations show that metal atoms preferentially sit at the center of the hexagons (H sites) just as in graphite. We first analyzed the structural deformation of BC_3 upon intercalation. As shown in Table 1, the optimized c value for Li, Na, and K intercalated BC_3 at different concentrations is, as expected, larger than the value for pristine BC_3, c = 3.08 Å. This value is largest for K intercalated BC_3 due to its larger van der Waals radius. This expansion, however, does not produce stress in the material as it occurs in the direction perpendicular to the layer plane. Along the plane, we find that the maximum increase in C−C and B−C bond lengths upon metal intercalation is between 2 and 5% for Li and Na and about 10% for K in K_2BC_3, which, as we show below, does not correspond to a stable stoichiometry.

Table 1. Optimized Interlayer Spacing (Å) for Different Stoichiometries of Li, Na, and K Intercalated BC_3

	M =		
stoichiometry	Li	Na	K
$M_{0.5}BC_3$	3.60	4.55	5.30
MBC_3	3.66	4.38	5.18
$M_{1.5}BC_3$	3.54	4.33	5.42
M_2BC_3	3.48	4.23	4.88

In order to study the stability of the intercalated compounds, we first calculated the binding energy of the different structures using the relation

$$xE_{\text{binding}} = E(M_xBC_3) - E(BC_3) - xE(M) \quad (1)$$

where $E(M_xBC_3)$, $E(BC_3)$, and $E(M)$ are the energies of M_xBC_3, pristine BC_3, and the metal atom in the pure bulk form, respectively. This binding energy directly compares the stability of M intercalated BC_3 with respect to its components, pristine BC_3 and metal bulk. According to its definition, a negative binding energy implies that the transformation $BC_3 + xM \rightarrow M_xBC_3$ is exothermic, where M_xBC_3 corresponds to an energetically favorable structure with respect to its constituents. The binding energies calculated for Li, Na, and K intercalated BC_3 in stage-I as a function of metal content are shown in Figure 2a. We also find that stage-II and stage-III of M_xBC_3 are stable with respect to its constituents. Our results are consistent with previously reported density-functional-theory-based values of Li intercalation in BC_3.[32] The differences in binding energies between our work and that previous work can be mostly

DOI: 10.1021/acs.jpclett.5b01110
J. Phys. Chem. Lett. 2015, 6, 2728−2732

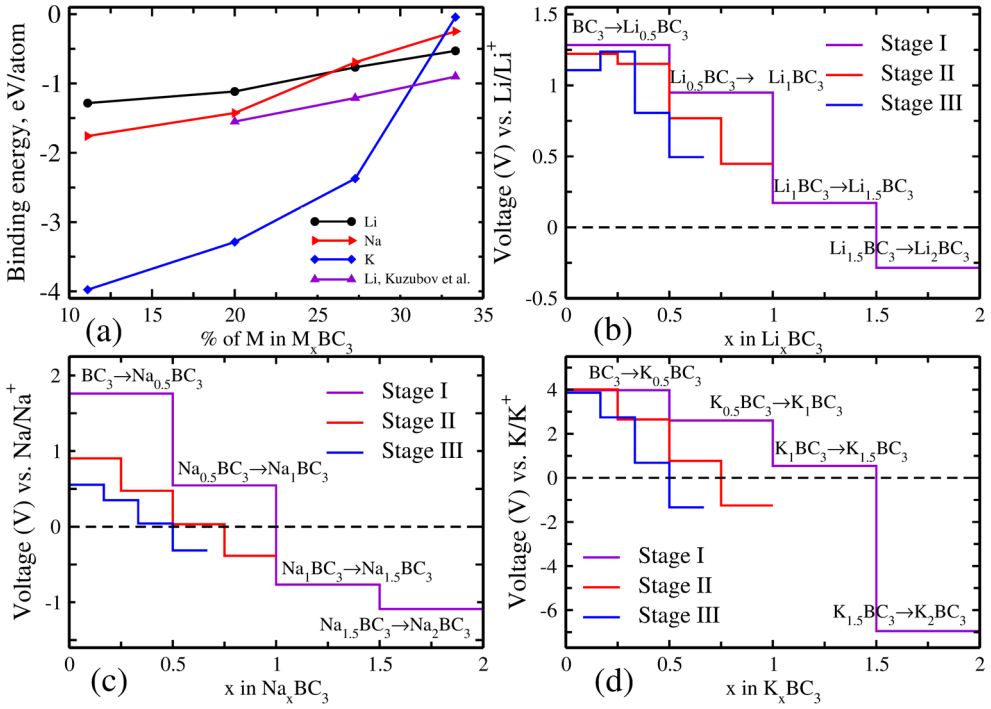

Figure 2. (a) Binding energy per M atom as a function of % of M atom in stage-I with respect to pristine BC_3 and bulk M. Upright triangles show previous results from Kuzubov et al.[32] Voltage profiles diagrams used to calculate the maximum intercalation capacity of M in layered BC_3 in stage-I, stage-II, and stage-III for (b) Li, (c) Na, and (d) K.

attributed to the different choice of exchange−correlation functional.

The maximum intercalation capacity for Li, Na, and K in BC_3 can be obtained from our calculations for the transformation

$$M_{x_0}BC_3 + (x - x_0)M \rightarrow M_xBC_3 \quad (2)$$

using the intercalation potential calculated by the relation[41]

$$V = -\frac{E(M_xBC_3) - E(M_{x_0}BC_3) - (x - x_0)E(M)}{x - x_0} \quad (3)$$

Equation 3 is defined in such a way that the maximum intercalation capacity corresponds to the stoichiometry beyond which the potential V becomes negative. For instance, the voltage profile diagrams shown in Figure 2b−d for stage-I represent the average intercalation potential for $BC_3 + 0.5M \rightarrow M_{0.5}BC_3$, $M_{0.5}BC_3 + 0.5M \rightarrow M_1BC_3$, $M_1BC_3 + 0.5M \rightarrow M_{1.5}BC_3$, and $M_{1.5}BC_3 + 0.5M \rightarrow M_2BC_3$. Although the maximum stoichiometry can be only obtained in stage-I (all galleries occupied), we also calculated the intercalation potential for stage-II and -III counterparts of all of the structures considered in stage-I to confirm the results obtained for stage-I (Figure 2).

The negative value of V for $Li_{1.5}BC_3 \rightarrow Li_2BC_3$ in Figure 2b implies that $Li_{1.5}BC_3$ cannot accept more Li to form Li_2BC_3 even though the Li binding energy of Li_2BC_3 is negative. These results indicate that Li_2BC_3 in stage-I is relatively unstable. Therefore, it is expected that in experiments, for larger concentrations than $Li_{1.5}BC_3$, Li will start precipitating to form dendrites (Li metal), which is detrimental for battery applications. The voltage profile diagrams for stage-II and stage-III show that even if Li_2BC_3 is not possible in stage-I, its stage-II and stage-III structures might be possible. This is due to the decreased repulsive interaction between the metal atom in different layers. Thus, for Li intercalation in BC_3, the maximum stable intercalation stoichiometry is $Li_{1.5}BC_3$, which corresponds to a theoretical capacity of 858 mA h/g, more than twice the capacity of graphitic anodes in LIBs.[24] These results are in good agreement with the previously reported work of Liu et al.[33]

In a similar way, we additionally studied the maximum intercalation capacity of Na and K in BC_3 by examining the voltage profile corresponding to the same four different stoichiometries considered in the case of Li intercalation. Negative intercalation potentials are found for stage-I $NaBC_3 \rightarrow Na_{1.5}BC_3$, indicating a maximum stable Na stoichiometry of $NaBC_3$. This same trend is maintained for stages-II and -III as well. We note that the very small intercalation potential corresponding to stage-II and stage-III of $Na_{1.5}BC_3 \rightarrow Na_2BC_3$ should be considered as zero as the DFT approximation employed slightly overestimates the potential of Li intercalation in graphite.[17] Thus, the maximum intercalation capacity corresponds to $NaBC_3$, which in terms of gravimetric capacity corresponds to 572 mA h/g, about twice as large as that of hard carbon in NIBs.[25] Likewise, it is clear from Figure 2d that the maximum intercalation capacity for K in BC_3 corresponds to the stoichiometry $K_{1.5}BC_3$ with a theoretical capacity of 858 mA h/g, about 3 times that of maximally loaded K in graphite[17] (KC_8).

We further investigated the voltage profile of M_xBC_3 corresponding to the maximum intercalated capacity calculated above. Voltage profiles for staged intercalation with maximum intercalated metal concentrations are shown in Figure 3. The first average voltage step corresponds to filling up the empty galleries to form a stage-III compound (herein denoted as $BC_3 \rightarrow$ III). The second step provides the average voltage of filling one more empty gallery, III → II. Finally, the last step corresponds to the average voltage for the transformation from stage-II to stage-I, denoted as II → I. From Figure 3, it is

DOI: 10.1021/acs.jpclett.5b01110
J. Phys. Chem. Lett. 2015, 6, 2728−2732

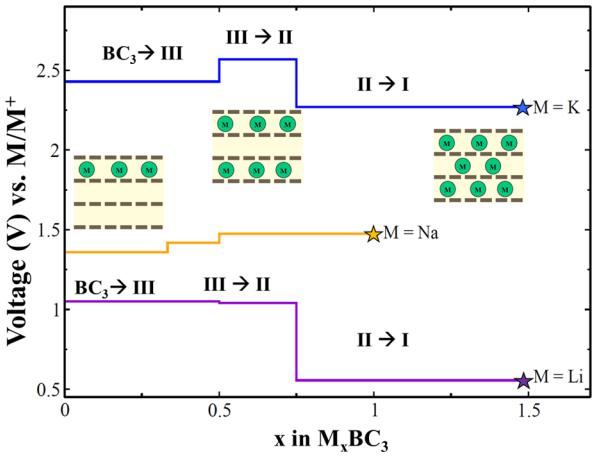

Figure 3. Staging voltage profile diagram for Li, Na, and K intercalation in BC_3. Stars indicate the calculated maximum theoretical capacity for each metal.

evident that the potential of the $Li_{1.5}BC_3$ electrode with respect to Li metal is in the range of 1.05−0.55 V, which is comparable to the experimentally observed potential of 1.25−0.10 V in LiC_6 graphite electrodes with respect to Li metal.[40] This voltage range provides an open-circuit voltage (OCV) of 2.95−3.45 V, fairly close to the OCV of Sony LIB (2.50 to 3.90 V)[32] by assuming a cathode electrode with a potential of 4 V showing the potential of the BC_3 anode material for LIBs.

Similarly, our results show that for sodium, up to a maximum stoichiometry of Na_1BC_3, the BC_3 electrode has an average potential in the range of 1.36−1.48 V, as shown in Figure 3. The calculated trend in the voltage profile presented here has also been reported experimentally for a graphitic anode[42] and for a Na electrode.[43] Like in the Li case, by using a cathode with a potential of ∼4 V with respect to metallic Na, for example, an OCV of 2.64−2.52 V is possible. Moreover, the calculated voltage variation of 0.12 V is smaller than that in a graphitic anode in a LIB (0.30 V), suggesting that this material is robust in terms of voltage stability. We believe that such a high voltage and small OCV variation in the proposed BC_3 anode could set a milestone for commercialization of NIBs.

Last, for the case of potassium, the calculated average potential for the maximally loaded BC_3 is in the range of 2.26−2.42 V. This high average potential of $K_{1.5}BC_3$ is not desirable for anode electrodes as it decreases significantly the OCV in a battery. We propose that K intercalated BC_3 could be used as a cathode material instead if combined with a low-voltage anode.

In conclusion, using energetic considerations based on dispersion-corrected density functional theory, we show that hexagonal BC_3 exhibits a great potential as an electrode material in metal ion batteries. Not only Li capacities in BC_3 are more than doubled with respect to graphite but, more importantly, BC_3 can reversibly intercalate Na and K up to a maximum capacity of 572 and 858 mA h/g, respectively. Our results show a striking contrast with graphitic carbon, which does not allow Na intercalation. BC_3 exhibits a small voltage variation upon charging and discharging, especially in the case of Na (0.12 V). We show that, compared to alkali metal intercalated graphite, alkali metal intercalated BC_3 is a much more robust material as it provides a larger M intake capacity and voltage stability and smaller structural changes during the charging and discharging process. Moreover, the small variation of voltage in M_xBC_3 with M concentration is an important feature of this material as it provides voltage stability while charging and discharging the electrode. Our results show that alkali metal intercalation in BC_3 presents all of the ingredients needed for robust electrodes and therefore encourage further experimental exploration.

■ ASSOCIATED CONTENT

Supporting Information

Information about computational details as well as additional results, including optimized bond lengths. The Supporting Information is available free of charge on the ACS Publications website at DOI: 10.1021/acs.jpclett.5b01110.

■ AUTHOR INFORMATION

Corresponding Author

*E-mail: baron1v@cmich.edu.

Notes

The authors declare no competing financial interest.

■ ACKNOWLEDGMENTS

V.B. gratefully acknowledges the support from NSF CBET-1335944. J.E.P. acknowledges support from NSF DMR-0906617 and DOE DE-FG02-10ER16203.

■ REFERENCES

(1) Armand, M.; Tarascon, J. M. Building Better Batteries. *Nature* **2008**, *451*, 652−657.
(2) Nagaura, T.; Tozawa, K. Lithium Ion Rechargeable Battery. *Prog. Batteries Sol. Cells* **1990**, *9*, 209−219.
(3) Noorden, R. V. The Rechargeable Revolution: A Better Battery. *Nature* **2014**, *507*, 26−28.
(4) Persson, K.; Hinuma, Y.; Meng, Y. S.; van der Ven, A.; Ceder, G. Thermodynamic and Kinetic Properties of the Li−Graphite System from First-Principles Calculations. *Phys. Rev. B* **2010**, *82*, 125416.
(5) Hou, J.; Shao, Y.; Ellis, M. W.; Moore, R. B.; Yi, B. Graphene-Based Electrochemical Energy Conversion and Storage: Fuel Cells, Supercapacitors and Lithium Ion Batteries. *Phys. Chem. Chem. Phys.* **2011**, *13*, 15384−15402.
(6) Tarascon, J.-M.; Armand, M. Issues and Challenges Facing Rechargeable Lithium Batteries. *Nature* **2001**, *414*, 359−367.
(7) Lee, E.; Persson, K. A. Li Absorption and Intercalation in Single Layer Graphene and Few Layer Graphene by First Principles. *Nano Lett.* **2012**, *12*, 4624−4628.
(8) Uthaisar, C.; Barone, V.; Fahlman, B. D. On the Chemical Nature of Thermally Reduced Graphene Oxide and Its Electrochemical Li Intake Capacity. *Carbon* **2013**, *61*, 558−567.
(9) Whittingham, M. S. Electrical Energy Storage and Intercalation Chemistry. *Science* **1976**, *192*, 1126−1127.
(10) Mizushima, K.; Jones, P.; Wiseman, P.; Goodenough, J. Li_xCoO_2 ($0 < x < 1$): A New Cathode Material for Batteries of High Energy Density. *Mater. Res. Bull.* **1980**, *15*, 783−789.
(11) Bareño, J.; Lei, C. H.; Wen, J. G.; Kang, S.-H.; Petrov, I.; Abraham, D. P. Local Structure of Layered Oxide Electrode Materials for Lithium-Ion Batteries. *Adv. Mater.* **2010**, *22*, 1122−1127.
(12) Longo, R. C.; Kong, F. T.; Santosh, K. C.; Park, M. S.; Yoon, J.; Yeon, D.-H.; Park, J.-H.; Doo, S.-G.; Cho, K. Phase Stability of Li−Mn−O Oxides as Cathode Materials for Li-Ion Batteries: Insights from Ab Initio Calculations. *Phys. Chem. Chem. Phys.* **2014**, *16*, 11233−11242.
(13) Mao, O.; Dunlap, R. A.; Dahn, J. R. Mechanically Alloyed Sn−Fe(−C) Powders as Anode Materials for Li-Ion Batteries: I. The Sn_2Fe−C System. *J. Electrochem. Soc.* **1999**, *146*, 405−413.
(14) Eames, C.; Islam, M. S. Ion Intercalation into Two-Dimensional Transition-Metal Carbides: Global Screening for New High-Capacity Battery Materials. *J. Am. Chem. Soc.* **2014**, *136*, 16270−16276.

DOI: 10.1021/acs.jpclett.5b01110
J. Phys. Chem. Lett. 2015, 6, 2728−2732

(15) Wang, Z.; Selbach, S. M.; Grande, T. Van der Waals Density Functional Study of the Energetics of Alkali Metal Intercalation in Graphite. *RSC Adv.* **2014**, *4*, 4069−4079.
(16) Kaloni, T.; Cheng, Y.; Kahaly, M. U.; Schwingenschlögl, U. Charge Carrier Density in Li-Intercalated Graphene. *Chem. Phys. Lett.* **2012**, *534*, 29−33.
(17) Okamoto, Y. Density Functional Theory Calculations of Alkali Metal (Li, Na, and K) Graphite Intercalation Compounds. *J. Phys. Chem. C* **2014**, *118*, 16−19.
(18) Nobuhara, K.; Nakayama, H.; Nose, M.; Nakanishi, S.; Iba, H. First-Principles Study of Alkali Metal−Graphite Intercalation Compounds. *J. Power Sources* **2013**, *243*, 585−587.
(19) Algdal, J.; Balasubramanian, T.; Breitholtz, M.; Kihlgren, T.; Walldén, L. Thin Graphite Overlayers: Graphene and Alkali Metal Intercalation. *Surf. Sci.* **2007**, *601*, 1167−1175.
(20) Billaud, D.; Henry, F.; Lelaurain, M.; Willmann, P. Revisited Structures of Dense and Dilute Stage {II} Lithium−Graphite Intercalation Compounds. *J. Phys. Chem. Solids* **1996**, *57*, 775−781.
(21) Chevallier, F.; Poli, F.; Montigny, B.; Letellier, M. In Situ ^{7}Li Nuclear Magnetic Resonance Observation of the Electrochemical Intercalation of Lithium in Graphite: Second Cycle Analysis. *Carbon* **2013**, *61*, 140−153.
(22) Yaroshevsky, A. Abundances of Chemical Elements in the Earth's Crust. *Geochem. Int.* **2006**, *44*, 48−55.
(23) Tofield, B. C.; Dell, R. M.; Jensen, J. Building Better Batteries. *Nature* **1978**, *276*, 217−218.
(24) Slater, M. D.; Kim, D.; Lee, E.; Johnson, C. S. Sodium-Ion Batteries. *Adv. Funct. Mater.* **2013**, *23*, 947−958.
(25) Komaba, S.; Murata, W.; Ishikawa, T.; Yabuuchi, N.; Ozeki, T.; Nakayama, T.; Ogata, A.; Gotoh, K.; Fujiwara, K. Electrochemical Na Insertion and Solid Electrolyte Interphase for Hard-Carbon Electrodes and Application to Na-Ion Batteries. *Adv. Funct. Mater.* **2011**, *21*, 3859−3867.
(26) Wan, W.; Wang, H. Study on the First-Principles Calculations of Graphite Intercalated by Alkali Metal (Li, Na, K). *Int. J. Electrochem. Sci.* **2015**, *10*, 3177−3184.
(27) Chevrier, V. L.; Ceder, G. Challenges for Na-Ion Negative Electrodes. *J. Electrochem. Soc.* **2011**, *158*, A1011−A1014.
(28) Whittingham, M. S. Chemistry of Intercalation Compounds: Metal Guests in Chalcogenide Hosts. *Prog. Solid State Chem.* **1978**, *12*, 41−99.
(29) Nishijima, M.; Gocheva, I. D.; Okada, S.; Doi, T.; ichi Yamaki, J.; Nishida, T. Cathode Properties of Metal Trifluorides in Li and Na Secondary Batteries. *J. Power Sources* **2009**, *190*, 558−562.
(30) Abraham, K. Intercalation Positive Electrodes for Rechargeable Sodium Cells. *Solid State Ionics* **1982**, *7*, 199−212.
(31) Xu, Q.; Ban, C.; Dillon, A. C.; Wei, S.-H.; Zhao, Y. First-Principles Study of Lithium Borocarbide as a Cathode Material for Rechargeable Li Ion Batteries. *J. Phys. Chem. Lett.* **2011**, *2*, 1129−1132.
(32) Kuzubov, A. A.; Fedorov, A. S.; Eliseeva, N. S.; Tomilin, F. N.; Avramov, P. V.; Fedorov, D. G. High-Capacity Electrode Material BC_3 for Lithium Batteries Proposed by Ab Initio Simulations. *Phys. Rev. B* **2012**, *85*, 195415.
(33) Liu, Y.; Artyukhov, V. I.; Liu, M.; Harutyunyan, A. R.; Yakobson, B. I. Feasibility of Lithium Storage on Graphene and Its Derivatives. *J. Phys. Chem. Lett.* **2013**, *4*, 1737−1742.
(34) Ling, C.; Mizuno, F. Boron-Doped Graphene as a Promising Anode for Na-Ion Batteries. *Phys. Chem. Chem. Phys.* **2014**, *16*, 10419−10424.
(35) Way, B. M.; Dahn, J. R. The Effect of Boron Substitution in Carbon on the Intercalation of Lithium in $Li_x(B_z C_{1-z})_6$. *J. Electrochem. Soc.* **1994**, *141*, 907−912.
(36) Kouvetakis, J.; Sasaki, T.; Shen, C.; Hagiwara, R.; Lerner, M.; Krishnan, K.; Bartlett, N. Novel Aspects of Graphite Intercalation by Fluorine and Fluorides and New B/C, C/N and B/C/N Materials Based on the Graphite Network. *Synth. Met.* **1990**, *34*, 1−7.
(37) Giannozzi, P.; Baroni, S.; Bonini, N.; Calandra, M.; Car, R.; Cavazzoni, C.; Ceresoli, D.; Chiarotti, G. L.; Cococcioni, M.; Dabo, I.; et al. QUANTUM ESPRESSO: A Modular and Open-Source Software Project for Quantum Simulations of Materials. *J. Phys.: Condens. Matter.* **2009**, *21*, 395502.
(38) Cooper, V. R. Van der Waals Density Functional: An Appropriate Exchange Functional. *Phys. Rev. B* **2010**, *81*, 161104.
(39) Ohzuku, T.; Iwakoshi, Y.; Sawai, K. Formation of Lithium−Graphite Intercalation Compounds in Nonaqueous Electrolytes and Their Application as a Negative Electrode for a Lithium Ion (Shuttlecock) Cell. *J. Electrochem. Soc.* **1993**, *140*, 2490−2498.
(40) Dahn, J. R. Phase Diagram of Li_xC_6. *Phys. Rev. B* **1991**, *44*, 9170−9177.
(41) Aydinol, M. K.; Kohan, A. F.; Ceder, G.; Cho, K.; Joannopoulos, J. Ab Initio Study of Lithium Intercalation in Metal Oxides and Metal Dichalcogenides. *Phys. Rev. B* **1997**, *56*, 1354−1365.
(42) Lin, M.-C.; Gong, M.; Lu, B.; Wu, Y.; Wang, D.-Y.; Guan, M.; Angell, M.; Chen, C.; Yang, J.; Hwang, B.-J. Building Better Batteries. *Nature* **2015**, *520*, 324−328.
(43) Nose, M.; Nakayama, H.; Nobuhara, K.; Yamaguchi, H.; Nakanishi, S.; Iba, H. $Na_4Co_3(PO_4)_2P_2O_7$: A Novel Storage Material for Sodium-Ion Batteries. *J. Power Sources* **2013**, *234*, 175−179.

DOI: 10.1021/acs.jpclett.5b01110
J. Phys. Chem. Lett. 2015, 6, 2728−2732